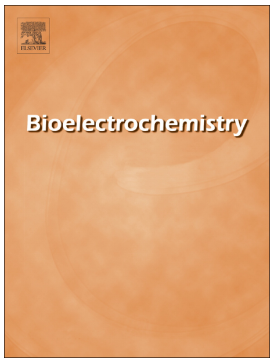

Interaction of DNA and mononucleotides with theophylline investigated using electrochemical biosensors and biosensing

Katarína Nemčeková, Ján Labuda, Viktor Milata, Jana Blaškovičová, Jozef Sochr

PII: S1567-5394(18)30070-7
DOI: doi:10.1016/j.bioelechem.2018.05.004
Reference: BIOJEC 7161

To appear in: *Bioelectrochemistry*

Received date: 9 February 2018
Revised date: 2 May 2018
Accepted date: 2 May 2018

Please cite this article as: Katarína Nemčeková, Ján Labuda, Viktor Milata, Jana Blaškovičová, Jozef Sochr , Interaction of DNA and mononucleotides with theophylline investigated using electrochemical biosensors and biosensing. The address for the corresponding author was captured as affiliation for all authors. Please check if appropriate. Biojec(2017), doi:10.1016/j.bioelechem.2018.05.004

Title: Interaction of DNA and mononucleotides with theophylline investigated using electrochemical biosensors and biosensing

Authors: Katarína Nemčeková[a, *], Ján Labuda[a, *], Viktor Milata[b], Jana Blaškovičová[a], Jozef Sochr[a]

Adresses: [a]Institute of Analytical Chemistry and [b]Institute of Organic Chemistry, Faculty of Chemical and Food Technology, Slovak University of Technology in Bratislava, 81237 Bratislava, Slovakia

Running head: DNA-theophylline interaction

Corresponding author: Professor Dr. Ján Labuda, D.Sc., Ing. Katarína Nemčeková

Institute of Analytical Chemistry, Faculty of Chemical and Food Technology,

Slovak University of Technology in Bratislava, Radlinského 9, 81237 Bratislava, Slovakia

E-mail: jan.labuda@stuba.sk, katarina.nemcekova@stuba.sk

Phone: +421-2-59325277, +421-918674277

Abstract

The understanding of DNA-drug interaction mechanism is among the important aspects of biological studies for drug design, discovery and pharmaceutical development processes. Published rather detailed FTIR and UV–visible spectroscopic studies on the interactions of theophylline, theobromine and caffeine with calf thymus DNA have shown effective binding of these methylxanthine derivatives to DNA and RNA involving H-bonds. However, to our knowledge, there is no such investigation using electrochemical approach. As a novelty of the study, in this paper the bioelectrochemical approach has been chosen for the investigation of an interaction of low molecular salmon sperm dsDNA, ssDNA and mononucleotides with theophylline (TP) in aqueous phosphate buffered medium using DNA-based electrochemical biosensors and biosensing in solution phase. Exploitation of the electrochemical approach via changes in square wave voltammetric responses of deoxyguanosine (dGuo) and deoxyadenosine (dAdo) provided a new indication on preferential association of TP with dGuo in the case of double helical dsDNA structure which was not reported previously. Moreover, an attachment of TP molecules outside DNA was found in the presence of high concentration of $3.3x10^{-4}$ M TP in solution which diminishes the electron transfer and leads to the difficulties in quantitative evaluation of the TP and dGuo voltammetric responses. The changes in UV-Vis and FTIR spectra obtained in the same medium confirmed the association interaction of TP with both nucleobases. Utilizing the model and the published energies of hydrogen bonding stabilization, the formation of a DNA-TP complex was predicted through the intermolecular H-bonds between TP and the NH-CO moiety of guanine and the $N-NH_2$ moiety of adenine.

Keywords: theophylline; DNA-based biosensor; DNA biosensing; DNA-drug interaction; square wave voltammetry; UV-Vis and IR spectrometry

1. Introduction

Exposure of deoxyribonucleic acid to endogeneous or exogeneous chemical and physical agents often leads to its non-covalent and covalent structural changes. Small inorganic and organic molecules of drugs and other chemicals can interact with DNA by various ways, e.g., through transcriptional factor, polymerase controlled RNA binding to DNA and non-covalent binding to the double helix. The later one can be performed by electrostatic binding between

positively charged guest and negatively charged DNA host, by binding to major and minor groove of DNA and by intercalation which means the insertion of the ligand molecule between base pairs [1]. Covalent changes may involve the interruption of chemical bonds in the DNA sugar phosphate backbone, resulting in the formation of single or double strand breaks or *N*-glycosidic bonds linking nucleobases to the sugar as well as their chemical modification. Investigation of a DNA-guest interaction helps us to enlighten the structural alterations of DNA and the action mechanism of guest molecules, for instance drugs [2].

Nowadays, these investigations are performed by various methods including spectrometry, electrophoresis, liquid and gas chromatography and also by electrochemical methods based on intrinsic response of the nitrogenous bases moieties after the interaction of DNA with guest molecules. The electrochemical studies of the DNA-guest interactions typically utilize electrodes with a surface-attached DNA (DNA-based biosensors) keeping the advantage of specificity, simplicity at operation, rapid response, potential miniaturized platform, low power requirement, and relatively low cost of the analysis [3-6]. Depending on a layer thickness of the chemical, such electrochemical sensors belong to the family of chemically modified electrodes characterized by quite thin film of the (bio)chemical modifier from a molecular monolayer to perhaps a few micrometers-thick multilayer [7] or to electrochemical biosensors having thick and often more complex layers of the biological recognition element [8]. At biosensing, the DNA-drug interaction is performed in a solution phase and subsequently detected electrochemically directly or after the immobilization of the reaction products at the working electrode [8].

Theophylline (TP) is known as a methylxanthine derivative which refers to alkaloid group found in black tea (about 7 $\mu g\ mL^{-1}$), cocoa beans (3.7 $mg\ g^{-1}$) and in traces in coffee and chocolate. TP has a stronger effect on the heart and breathing than caffeine and is used medically for treating respiratory and cardiovascular diseases as chronic obstructive pulmonary disease [9]. Its chemical structure is similar to that of nucleobases and other methylxanthines, especially to caffeine (Scheme 1).

Nowadays, rather limited number of reports on the DNA-methylxanthines interactions can be found. The study of the DNA-caffeine interaction at high concentration of caffeine using infrared linear dichroism demonstrated an arrangement of caffeine molecules outside the DNA double helix with an orientation parallel to the bases and that intercalation is not the predominant mechanism [10]. Time Correlated Single Photon Counting (TCSPC) was used to analyze the changes in the mode of intercalation of ethidium bromide and acridine orange to

calf thymus DNA brought about due to interaction with methylxanthines such as TP, theobromine and caffeine [11]. Hetero-association constants of TP with various biologically active aromatic compounds such as daunomycin, novantrone, ethidium bromide, proflavine, norfloxacin and the complexation constants of TP with both single- and double-stranded oligonucleotides in solution were determined by ^{1}H NMR measurements and the quantitative estimation of the effect of TP on binding of the aromatic ligands with DNA was reported [12]. The interaction of calf thymus dsDNA [13] and herring sperm DNA [14] with TP was investigated in details by the UV-Vis and FTIR spectroscopy. According to these studies, the bindings of caffeine and TP to nucleic acids exhibit a dose dependent behaviour and the complexation occurs through H-bonding with the G-C and A-T nucleobases and the PO_2 group. It was stated that the absence of methyl group bound at the N_7 site of 5-membered ring found in caffeine allows TP to form coordinates with double helical DNA and TP shows greater binding efficacy than caffeine [13] or similar one in order "caffeine≥theophylline>theobromine" [14]. The DNA conformation up to aggregation changes have been also found to depend on the concentration ratio of TP and DNA [13]. From this point of view the utilization of electrochemical signals of TP and nucleobases at these investigations should be of interest. However, an electrochemical investigation of direct DNA-TP interactions has not been fully performed.

In difference to the published spectroscopic studies, in this paper the bioelectrochemical approach has been chosen as a novelty of the DNA-TP study. The aim of this work was a characterization the interaction and binding mode of TP to low molecular salmon sperm dsDNA, ssDNA and mononucleotides using electrochemical measurements with the DNA-based biosensors and biosensing and verification of the results obtained by UV-Vis and FTIR investigations in the same medium.

2. Materials and methods

2.1. Apparatus

Voltammetric measurements were performed using the Metrohm/Eco Chemie Autolab PGSTAT12 Potentiostat/Galvanostat Electrochemical System (Eco Chemie, Netherlands) driven by the software NOVA version 1.10.23 (Metrohm Autolab, Netherlands). Graphical analysis was performed in software OriginPro 8.0. A three-electrode system composed of glassy carbon working electrode (GCE) with a disc diameter of 3 mm (Metrohm, Netherlands), a silver/silver chloride reference electrode (Ag/AgCl/salt KCl, L-CHEM, Czech

Republic) and a platinum counter electrode was used. Phosphate buffer solution (PB, pH 7.4; 0.1 M) was used as a supporting electrolyte. The experiments were performed in a 10 ml glass cells. UV-VIS spectrometric analysis was performed by spectrophotometer Thermo Scientific-Evolution 201 (USA) with quartz cuvettes. FTIR absorption spectra were recorded on Perkin-Elmer FTIR spectrometer Spectrum Two UTa (ZnSe). All experiments were carried out at ambient temperature.

2.2. Reagents

TP was purchased from Sigma Aldrich (Slovakia). Its stock solution of 1 mg mL^{-1} was prepared in PB by sonicating over 5 min, then stirring over 1 hour at 60°C, and stored at 4°C. Salmon sperm dsDNA was purchased from Sigma Aldrich (Slovakia) and its 0.1 $mg.mL^{-1}$ stock solution in PB was stored at 4°C. The molar concentration of dsDNA of $6.1x10^{-5}$ M (in base pairs, bp) was determined spectrophotometrically at 278 nm using molar absorption coefficient as 6600 M^{-1} cm^{-1}. The solution of ssDNA was prepared from stock solution of salmon sperm dsDNA by boiling dsDNA solution over 15 min and thereafter by quick and intense cooling in ice bath. 2′-Deoxyadenosine 5′-monophosphate and 2′-Deoxyguanosine 5′-monophosphate were purchased from Sigma Aldrich (Slovakia). Their stock solutions were prepared by dissolving in PB and stored at 4°C.

2.3. Preparation of DNA-based biosensor

The GCE surface was first cleaned mechanically by polishing with “alumina slurry” 0.3 μm (Metrohm, Netherlands) applied to mohair paper, washed with nanopure water and pre-treated by applying a potential of +1.7 V for 300 s in PB under stirring. A voltammetric control scan in 1 mM redox indicator $[Fe(CN)_6]^{3-/4-}$ was performed to monitor the quality of the bare working electrode. To fabricate the biosensor, a drop volume of dsDNA stock solution or ssDNA solution was introduced on the GCE surface and dried.

Alternatively, at biosensing, a drop volume of solution of the DNA and TP reaction mixture was applied to the electrode surface and evaporated to dryness during 15 min under open air conditions. The prepared chemically modified GCE were immersed into PB for 2 min under stirring to achieve equilibrium.

2.4. Procedures

Cyclic voltammograms of 1 mM $[Fe(CN)_6]^{3-/4-}$ were obtained using potential range -0.4 V to +0.8 V, scan rate 150 mV s^{-1}, potential step 2 mV. Square wave voltammograms were recorded in test solutions of TP (using the biosensors) or in 0.1 M PB pH 7.4 (using

biosensing) within a potential range from +0.0 V to +1.5 V, scan rate 255 mV s^{-1}, amplitude 0.04 V, potential step 25.5 mV, frequency 10 Hz.

UV-VIS absorption spectra were obtained within the wavelength rage from 240 nm to 320 nm. FTIR spectra were recorded in the region from 4000 cm^{-1} to 500 cm^{-1}.

3. Results and discussion

3.1. Electrochemical study of the DNA-TP interaction using DNA-based biosensor

Electrochemical behaviour of TP at bare GCE

Using the cyclic voltammetry (CV), $1.7x10^{-4}$ M TP in 0.1 M PB exhibited irreversible oxidation at the GCE with a diffusion controlled anodic peak at about 1.05 V where the maximum current linearly increased with the scan square root for the scan rates from 25 to 200 mV s^{-1} at a peak potential shifted by about 20 mV to positive potential values.

Using the square-wave voltammetry (SWV), the TP possessed the peak at 0.95 V which could be detected at the concentrations higher than $5.6.10^{-6}$ M. An appearance of the TP voltammetric signal in the given potential region should be taken into account as a potential interference to the anodic voltammetric signal of the dGuo moiety of nucleic acids.

Electrochemical behaviour of TP at dsDNA/GCE

At the DNA-based biosensors generally, the $[Fe(CN)_6]^{3-/4-}$ complex anion is typically used as the redox indicator to test the presence and quality of the DNA layer. Due to a repulsion of the indicator anions by the negatively charged DNA backbone, a decrease in the $[Fe(CN)_6]^{3-/4-}$ signal is observed when compared to that at a bare electrode without DNA [8]. The incubation of the dsDNA/GCE biosensor in $1.7x10^{-4}$ M TP for 5 min has caused a further significant decrease of the $[Fe(CN)_6]^{3-/4-}$ CV peak current (Fig. 1a). It indicates an additional barrier effect for the electron transfer between the redox indicator in the solution phase and the electrode surface caused evidently by a DNA-TP association and/or other behaviour of TP itself in high molar excess to the surface-attached dsDNA. Such behaviour can be ascribed to an arrangement of TP molecules outside the DNA backbone similarly to that reported for caffeine [10].

On the other hand, however, no change of the $[Fe(CN)_6]^{3-/4-}$ CV picture was observed after the incubation of dsDNA/GCE in low TP concentration of $5.6x10^{-7}$ M (Fig 1b) indicating that

such a low concentration of TP (where adsorption neither on the bare GCE nor on dsDNA/GCE is observed and the SWV response of TP is still negligible) should be suitable for an evaluation of its interaction with the nucleobases.

Therefore, the low TP concentration of $5.6x10^{-7}$ M and sensitive SWV technique have been chosen for the further investigation of the nucleobase-TP interaction. The dsDNA/GCE exhibited SWV peaks of deoxyguanosine (dGuo, at 1.05 V) and deoxyadenosine (dAdo, at about 1.3 V) with higher response of dAdo comparing to that of dGuo as typically [15-17]. At the incubation of the biosensor in the $5.6x10^{-7}$ M TP solution, the peak of dGuo showed a progressive decrease with time up to about 5 min incubation time (Fig. 2). This incubation time was used in some further experiments. Moreover, a slight shift of the dGuo peak by about 50 mV to more negative potential values was detected which indicates an energetically simpler oxidation (an opposite peak potential shift to more positive potential values is sometimes used as the indication of interaction by intercalation [18]). The original SWV peak corresponding to the dAdo oxidation was practically not changed in height but exhibited also some negative potential shift (Fig. 2).

Electrochemical behaviour of TP at ssDNA/GCE

In order to investigate deeply the DNA-drug interaction, single stranded derivative of salmon sperm DNA was prepared by the denaturation of dsDNA and used as well. The nucleobases of original ssDNA produce the anodic peaks of higher current values comparing to those of dsDNA (Figs. 2 and 3) because of a better steric access for an electron transfer from the single strand [8]. A significant decrease of the SWV peaks of both dGuo and dAdo without a potential shift was detected after the incubation of ssDNA/GCE in low TP concentration (Fig. 3a) thus indicating an interaction of both nucleobases with TP. This is a difference to behaviour observed at the closed structure of dsDNA that indicated preferential binding of TP to dGuo.

A decrease in the dAdo peak was also observed using relatively high TP concentration of $3.3x10^{-4}$ M (Fig. 3b) where, however, the peak of dGuo is overlapped with that of TP being in large molar excess. The significant decrease in the TP response comparing to bare GCE (full blue line compared to dashed blue line) indicates lower access of the depolarizer (here TP) to the electron transfer due to binding with the ssDNA layer similarly as it was found in CV of the redox indicator $[Fe(CN)_6]^{3-/4-}$ (Fig. 1a). It can mean again an arrangement of TP molecules outside the ssDNA backbone.

3.2. Electrochemical biosensing of the interaction of dsDNA, ssDNA and mononucleotides with TP in solution

To verify the results obtained with the electrochemical DNA-based biosensors, the DNA-drug interaction was performed in a solution followed by coating of the bare GCE surface with a small amount of the reaction mixtures of TP with dsDNA, ssDNA and mononucleotides, resp. After evaporation to dryness, the chemically modified electrode formed was incubated in PB solution to achieve equilibrium and the SWV signals of the nucleobases residues were recorded.

For these experiments relatively high concentrations TP and nucleic acids were chosen in order to obtain proper values of their SWV responses as at the biosensors. The interaction of nucleic acids with $3.3x10^{-4}$ M TP was performed in solutions with the molar ratio dsDNA(bp)/TP = 1/0.2 and ssDNA(bp)/TP = 1/1. Several reaction time intervals have been tested from 5 min to 24 h with no effect of the duration. The interval of 15 min has been chosen for both the DNA+TP mixtures incubation and the evaporation of their mixture at the electrode surface to dryness. The corresponding SWV curves are depicted in Fig. 4. Similarly to the behaviour at the dsDNA/GCE biosensor (Fig. 2), a significant decrease of the dGuo response and no change in the dAdo response were found for the TP mixture with dsDNA (Fig. 4a). In the case of mixture ssDNA plus TP, a decrease of the dAdo response has been also recorded (Fig. 4b) similarly to the behaviour observed at the ssDNA/GCE biosensor (Fig. 3). The signal of dGuo was, however, affected by the electrochemical and binding interference with the response of TP when their joint peak (full blue line) is much lower than that obtained for TP itself at GCE (dashed blue line) thus confirming the TP association interaction outside ssDNA and blocking of the electron transport.

A separate investigation of the TP interaction with individual nucleobases was performed using deoxyadenosine monophosphate (dAMP) and deoxyguanosine monophosphate (dGMP). The SWV curve registered after the dAMP-TP interaction (Fig. 4c) confirmed association of the reaction partners when the TP response at 0.95 V clearly diminished (blue full line) comparing to that at the bare GCE (blue dashed line) and the dAdo response decreased with increasing TP concentration. Using dGMP (Fig. 3d), the interference of the dGuo and TP peaks leads to a cumulated (dGuo + TP) response under a small peak shift to the higher potential values. This peak covers a decrease in both dGuo and TP responses with increased TP concentration.

A decrease in voltammetric responses of the nucleobases are typically evaluated in the DNA-drug interaction studies and, according to other various experimental evidences, ascribed to different modes of the association interaction. Recent examples of a significant decrease in nucleobases responses after the interaction with drugs are presented in Table 1. Similarly to the results observed here, a preferential decrease in the dGuo signal has been found in [15, 17, 19], H-bonding in [25] and binding outside the duplex in [27]. In all cases, however, the redox signals of the drugs were situated far from the oxidation responses of the nucleobases and did not interfere.

Table 1 DNA-drug interactions accompanied with a decrease of the nucleobases moieties electrochemical response

Drug	Electrode*	Conditions	Interaction	Ref.
anthramycin	HDME, peak G	0.3 M ammonium formate + 50 mM phosphate buffer pH 6.9	covalent bonding	[19]
aripiprazole	Multilayer dsDNA/GCE	0.1 M acetate buffer pH 4.5	binding to DNA bases	[15]
calcium dobesilate	dsDNA and ssDNA/AuNPs/ GCE	0.1 M phosphate buffer pH 6.0	intercalation	[20]
capsaicin	dsDNA/PGE	0.5 M acetate buffer pH 4.8 with 0.02 M NaCl	intercalation (competition with ethidium bromide)	[21]
metallo-drugs	dsDNA/SPE	5 mM phosphate buffer pH 7.4	covalent bonding	[22]
danusertib	dsDNA/GCE	0.1 M acetate buffer pH 4.5	electrostatic interaction	[17]
lapatinib	dsDNA/GCE	0.1 M acetate buffer pH 4.70	intercalation	[18]
leuprolide	dsDNA/PGE	0.5 M acetate buffer pH 4.8 with 0.02 M NaCl	binding to guanine	[23]
Mannich bases	dsDNA/PGE	0.5M acetate buffer pH 4.8 with 0.02 M NaCl	intercalation, alkylation	[24]
methotrexate	dsDNA/GCE	acetate buffer pH 4.2 (20% ethanol)	intercalation, electrostatic interaction and H-bonding	[25]
taxol (paclitaxel)	dsDNA/PGE	acetate buffer pH 4.8 with 0.02 M NaCl	intercalation	[26]
riboflavine	dsDNA/PGE	Tris buffer pH 7.0	binding to DNA bases and outside duplex	[27]

temozolomide	Multilayer dsDNA/GCE	0.1 M phosphate buffer pH 7.4	condensation of double helix	[28]

* HDME – hanging mercury drop electrode, GCE- glassy carbon electrode, PGE - pencil graphite electrode, SPE - screen printed electrode

3.3. Spectrometric study of the dsDNA-TP interaction

UV-Vis absorption spectra

UV–Vis spectrometry is the very common technique to study the interaction between nucleic acids and small molecules. Fig. 5 shows UV-Vis absorption spectra for three different concentrations of TP and corresponding mixtures with dsDNA of the constant concentration (in some excess of the base pairs concentration to TP in the ratio of about 5.6, 2.2 and 1.1) and the typical absorption band of the nucleobases at 260 nm (red lines). The absorbance of TP itself at 272 nm (blue lines) increased with its concentration. The dsDNA-TP mixtures (green lines) exhibited rather complex spectra with a large band situated between the bands of the individual components (DNA and TP) regarding both, the wavelength position and the absorbance value depending on the TP concentration. This complex band shows an increase in the absorbance with the bathochromic shift to longer wavelengths similarly to [14] where the hyperchromicity at the 260 nm wavelength with increasing phosphate-drug ratio from 6 to 0.8 was found. However, the difference spectra (brown lines) obtained here by software subtracting the corresponding absorbance of TP from those of the dsDNA-TP mixtures clearly show a decrease in the absorbance value (hypochromic effect) of the nucleobases band with a slight blue (hypsochromic) shift (about 7 nm) with increasing concentration of TP. These spectral changes demonstrate TP binding to the nucleobases of dsDNA and the formation of a dsDNA-TP complex. The UV-Vis spectral changes reported in the study of calf thymus dsDNA with caffeine and theophylline under similar concentrations of the free DNA and the drugs [13] reported an increase in intensity of the TP characteristic UV-Vis band at 278 nm which was ascribed to major drug-DNA interaction at the DNA surface not limiting the mobility of the TP around DNA molecule. Generally, the hypochromicity at the maximum absorbance of DNA (260 nm) indicates the compactation of DNA due to the electrostatic interaction while intercalation mechanism induces the hyperchromicity at this wavelength [29].

FTIR spectra

An evidence for the DNA–TP complexation comes also from the infrared spectroscopic study typically used to determine drug binding sites, sequence preference, DNA secondary

structure, and the structural variations in DNA-drug complexes [30]. To verify the results of electrochemical investigations, FTIR spectra were obtained with dsDNA and TP in mM concentration range under experimental conditions used at the electrochemical study. Fig. 5 shows the IR spectra recorded for dsDNA, TP, and their mixture with the concentration ratio of dsDNA (in bp) to TP equal 3:1 in PB solution. According to [31-34], individual absorption bands can be ascribed as follows: 1737 a 1725 cm^{-1} to guanine (G) and thymine (T) C=O stretching, 1638 cm^{-1} to adenine (A) C_7=N stretching, 1481 a 1439 cm^{-1} to cytosine (C) vibration, 1366 cm^{-1} to all nucleobases, 1216 cm^{-1} to DNA phosphate antisymmetric stretching, 1085 cm^{-1} to DNA phosphate symmetric stretching and 953 cm^{-1} to D-ribose.

The absorption bands of nucleobases for the dsDNA–TP mixture strongly diminished in the corresponding regions from 1737 to 1725 cm^{-1} and 1481 to 1353 cm^{-1} confirming the DNA–drug interaction as well as DNA helix structural change. The unchanged band of A at 1638 cm^{-1} is due to overlapping with the absorption of TP alone (with the C=O stretching band at 1714 cm^{-1}, C=C and C=N stretching modes at 1666–1650 cm^{-1} [13]). At the same time, the bands shifts to higher wavenumbers (for G from 1737 to 1759 cm^{-1}, T from 1725 to 1734 cm^{-1} and C from 1481 to 1484 cm^{-1}) were observed. Similar shifts in the vibrational frequencies were reported as the clear indication of the methylxanthine drug interaction with the A-T and G-C bases where the NH and CO groups of DNA and the drugs are mutually involved in H-bonding [14]. The PO_2 bands exhibited only a strong decrease in the vibrational intensities which indicates again a TP interaction with the DNA backbone.

Based on the results obtained, we can presume the interaction of TP with the guanine moiety through the free electron pair of the carbonyl oxygen C_6=O (electron donor) and tautomeric N_7-H (H-donor) exploiting the known G-C base-pair model from the DNA double helix structure based on hydrogen bonding to NH-CO moiety of guanine (Scheme 2a, left) or to the enol form of guanine (Scheme 2a, right). The oxo-form of dGuo is generally more stable by about 37.7 kJ mol^{-1}. Using the enthalpies of various hydrogen bonds OH···N (28.9 kJ mol^{-1}), NH···N (13 kJ mol^{-1}), NH···O (8 kJ mol^{-1}) and OH···O (20.9 kJ mol^{-1}) [35] we obtain the value about 19.7 kJ mol-1 which prefers the left structure.

For the interaction of TP to dAdo practically only one structure is coming on force which is displayed on Scheme 2b. Exploring this picture from the point of view of the previously used energies, the association interaction gives the smallest stabilisation which corresponds well with experimental data that the guanine moiety is interacting preferentially in comparison to adenine.

4. Conclusion

Use of spectroscopic and electrochemical approaches typically possesses complex information from the biomolecules interaction studies. Till now, the DNA-TP interaction has been investigated dominantly spectrometrically. In this novel study, the bioelectrochemical investigations performed for the first time have confirmed the association interaction of TP with nucleobases at the surface of the dsDNA and ssDNA-based biosensors as well as in solution of dsDNA, ssDNA, and guanosine and adenosine monophosphates. Exploitation of the bioelectrochemical approach provided via changes in square wave voltammetric responses of dGuo and dAdo new indication on preferential association of TP with dGuo in the case of closed structure of dsDNA. Moreover, some fixation of TP outside DNA has been also found which limits the charge transfer to electrode and its response. These properties were confirmed by UV-Vis and FTIR analyses and are in agreement with the spectrometric studies published previously. In accordance with the published reports, close structural similarities of the nucleobases and methylxanthines lead to interferences of their responses at both the electrochemical and spectrometric investigations. For this reason, two different concentration levels of TP were used together with the separate investigation of dGuo and dAdo responses. Nevertheless, the redox interference between TP and dGuo evidently caused some bias in the response values which allowed rather qualitative evaluation of the interaction and not the calculation of the binding constants.

Exploiting the known base-pairing model from the DNA double helix structure based on hydrogen bonding, the interaction models were proposed for binding of TP to NH-CO moiety of guanine and to N-NH_2 moiety of adenine which correspond well with experimental data. The guanine moiety is interacting with TP preferentially in comparison to adenine. Such intermolecular nucleobase-TP associations follow also from the known energies of the structure stabilization by different types of the hydrogen bonds.

Declaration of interest. Acknowledgements

The authors report no conflicts of interest. The authors alone are responsible for the content of the paper. This work was supported by the Scientific Grant Agency VEGA of the Slovak Republic (Project No. 1/0489/16) and the Slovak Research and Development Agency under the Contract No. APVV-0797-11.

References

1. E. Paleček, M. Bartošík, Electrochemistry of Nucleic Acids, Chem. Rev. 112 (2012) 3427–3481.
2. M. Sirajuddin, S. Ali, A. Badshah, Drug-DNA interactions and their study by UV-Visible, fluorescence spectroscopies and cyclic voltammetry, J. Photochem. Photobiol. B. 124 (2013) 1-19.
3. M. Fojta, A. Daňhel, L. Havran, V. Vyskočil, Recent progress in electrochemical sensors and assays for DNA damage and repair, Trends Anal. Chem. 79 (2013) 160-167.
4. S. Kurbanoglu, B. Dogan-Topal, E. P. Rodriguez, B. Bozal-Palabiyik, S. A. Ozkan, B. Uslu, Advances in electrochemical DNA biosensors and their interaction mechanism with pharmaceuticals, J Electroanal. Chem. 775 (2016) 8-26.
5. V. C. Diculescu, A. M. Chiorcea-Paquim, A. M. Oliveira-Brett, Applications of a DNA-electrochemical biosensor. Trends Anal. Chem. 79 (2016) 23-36.
6. V. Svitková, J. Labuda, Construction of electrochemical DNA biosensors for investigation of potential risk chemical and physical agents, Chemical Monthly 148 (2017) 1569–1579.
7. R. A. Durst, A. J. Baumner, R. W. Murray, R. P. Buck, C. P. Andrieux, Chemically modified electrodes: Recommended terminology and definitions (IUPAC Recommendations 1997), Pure Appl. Chem. 69 (1997) 1317-1323.
8. J. Labuda, A. M. O. Brett, G. Evtugyn, M. Fojta, M. Mascini, M. Ozsoz, I. Palchetti, E. Paleček, J. Wang, Electrochemical nucleic acid-based biosensors: Concepts, terms and methodology (IUPAC Technical Report), Pure Appl. Chem. 82 (2012) 1161-1187.
9. K. Cinková, N. Zbojeková, M. Vojs, M. Marton, A. Samphao, Ľ. Švorc, Electroanalytical application of a boron-doped diamond electrode for sensitive voltammetric determination of theophylline in pharmaceutical dosages and human urine, Anal. Methods 7 (2015) 6755-6763.
10. H. Fritzsche, H. Lang, H. Sprinz, W. Pohle, On the interaction of caffeine with nucleic acids: IV. Studies of the caffeine-DNA interaction by infrared and ultraviolet linear dichroism, proton and deuteron nuclear magnetic resonance, Biophys. Chem. 11 (1980) 121-131.
11. M. Johnson, S.G. Bhuvan Kumar, R. Malathi, De-intercalation of ethidium bromide and acridine orange by xanthine derivatives and their modulatory effect on anticancer agents: a

study of DNA-directed toxicity enlightened by time correlated single photon counting. J. Biomol. Struct. & Dyn. 20 (2003) 677-685.

12. A. A. Hernandez Santiago, D. D. Andrejuk, A. M. Cervantes Tavera, D. B. Davies, M. P. Evstigneev, Complexation of biologically active aromatic compounds with DNA in the presence of theophylline, J Biol Phys. 35 (2009) 115-126.
13. S. Nafisi, F. Manouchehri, H. Tajmir-Riahi, M. Varavipour, Structural features of DNA interaction with caffeine and theophylline, J. Mol. Struct. 875 (2008) 392-399.
14. I. M. Johnson, H. Prakash, J. Prathiba, R. Raghunathan, R. Malathi, Spectral Analysis of Naturally Occurring Methylxanthines (Theophylline, Theobromine and Caffeine) Binding with DNA, Plos One 7 (2012) 1-11.
15. S. Kurbanoglu, B. Dogan-Topal, L. Hlavatá, J. Labuda, S. A. Ozkan, B. Uslu, Electrochemical investigation of an interaction of the antidepressant drug aripiprazole with original and damaged calf thymus dsDNA, Electrochim. Acta 169 (2015) 233-240.
16. A. M. O. Brett, L. A. da Silva, C. M. A. Brett, Adsorption of guanine, guanosine and adenine at electrodes studied by differential pulse voltammetry and electrochemical impedance, Langmuir 18 (2002) 2326-2330.
17. V. C. Diculescu, A. M. O. Brett, In situ electrochemical evaluation of dsDNA interaction with the anticancer drug danusertib nitrenium radical product using the DNA-electrochemical biosensor, Bioelectrochem. 107 (2016) 50-57.
18. B. Dogan-Topal, B. Bozal-Palabiyik, S. A. Ozkan, B. Uslu, Investigation of anticancer drug lapatinib and its interaction with dsDNA by electrochemical and spectroscopic techniques, Sens. Actuator B-Chem. 194 (2014) 185-194.
19. C. Teijeiro, E. de la Red, D. Marin, Electrochemical Analysis of Anthramycin: Hydrolysis DNA-Interactions and Quantitative Determination, Electroanalysis. 12 (2000) 963-968.
20. H. Xu, X. Li, J. Zhang, K. Liu, Electrochemical studies of calcium dobesilate and interaction with DNA, Microchim. Acta 165 (2009) 415-420.
21. N. Yilmaz, E. Eksin, B. Karacicek, Y. Erac, A. Erdem, Electrochemical detection of interaction between capsaicin and nucleic acids in comparison to agarose gel electrophoresis, Anal. Biochem. 535 (2017) 56-62.
22. M. Mascini, G. Bagni, M. L. Di Pietro, M. Ravera, S. Baracco, D. Osella, Electrochemical biosensor evaluation of the interaction between DNA and metalo-drugs, BioMetals. 19 (2006) 409-418.

23. B. Dogan-Topal, S. A. Ozkan, A novel sensitive electrochemical DNA biosensor for assaying of anticancer drug leuprolide and its adsorptive stripping voltammetric determination, Talanta. 83 (2011) 780-788.

24. H. Istanbullu, H. Karadeniz, E. Erciyas, A. Erdem, Electrochemical detection of DNA interaction with mannich base derivatives by disposable graphite electrodes, Turk. J. Chem. 41 (2017) 40-47.

25. B. Rafique, A. M. Khalid, K. Akhtar, A. Jabbar, Interaction of anticancer drug methotrexate with DNA analyzed by electrochemical and spectroscopic methods, Biosens. Bioelectron. 44 (2013) 21–26.

26. S. Tajik, M. A. Taher, H. Beitollahi, M. Torkzadeh-Mahani, Electrochemical determination of the anticancer drug taxol at a ds-DNA modified pencil-graphite electrode and its application as a label-free electrochemical biosensor, Talanta. 134 (2015) 60-64.

27. A. A. Ensafi, E. H. Bafrooei, M. Amini, DNA-functionalized biosensor for riboflavin based electrochemical interaction on pretreated pencil graphite electrode, Biosens. Bioelectron. 31 (2012) 376-381.

28. I. Lopes, S. C. Oliveira, A. M. Oliveira-Brett, In situ electrochemical evaluation of anticancer drug temozolomide and its metabolites-DNA interaction, Anal. Bioanal. Chem. 405 (2013) 3783-3790.

29. R. Hajian, P. Hossaini, Z. Mehrayin, P. M. Woi, N. Shams, DNA-binding studies of valrubicin as a chemotherapy drug using spectroscopy and electrochemical techniques, J. Pharm. Anal. 7 (2017) 176-180.

30. J. M. Le Gal, H. Morjani, M. Manfait, Ultrastructural appraisal of the multidrug resistance in K562 and LR73 cell lines from fourier transform infrared spectroscopy, Cancer Research. 53 (1993) 3681-3686.

31. S. Charak, D. K. Jangir, G. Tyagi, R. Mehrotra, Interaction studies of Epirubicin with DNA using spectroscopic techniques, J. Mol. Struct. 1000 (2011) 150-154.

32. S. T. Saito, G. Silva, C. Pungartnik, M. Brendel, Study of DNA-emodin interaction by FTIR and UV-vis spectroscopy, J. Photochem. Photobiol. B-Biol. 111 (2012) 59-63.

33. M. Luiza, S. Mello, B. C. Vidal, Changes in the Infrared Microspectroscopic Characteristic of DNA Caused by Cationic Elements, Different Base Richness and Single-Stranded Form, Plos One. 7 (2012) 1-12.

34. N. A. Elmarzugi, T. Adali, A. M. Bentaleb, E. I. Keleb, A. T. Mohamed, A. M. Hamza, Spectroscopic Characterization of PEG-DNA Biocomplexes by FTIR, J. Appl. Pharm. Sci. 4 (2014) 6-10.

35. O. Markovitch, N. Agmon, Structure and energetics of the hydronium hydration shells, J. Phys. Chem. A. 111 (2007) 2253-2256.

Caption to figures

Scheme 1 Chemical structure of theophylline (left) and caffeine (right)

Scheme 2 Proposed models for the interaction of TP with guanine (a) and adenine (b) moieties

Fig. 1 Cyclic voltammograms of $1x10^{-3}$ M $[Fe(CN)_6]^{3-/4-}$ in 0.1 M PB pH 7.4 at bare GCE before (black line) and after incubation in TP (blue line), and at dsDNA/GCE before (red line) and after incubation in TP (green line), $1.7x10^{-4}$ M TP (a) and $5.6x10^{-7}$ M TP (b), scan rate 150 mV s^{-1}

Fig. 2 Baseline-corrected SWV responses of dGuo and dAdo after the incubation of dsDNA/GCE in $5.6x10^{-7}$ M TP for given time, recorded in the same solution, scan rate 255 mV s^{-1}

Fig. 3 Baseline-corrected SWV responses of dGuo and dAdo after 5 min incubation of ssDNA/GCE in $5.6x10^{-7}$ M (a) and in $3.3x10^{-4}$ M (b) TP, recorded in the same solution. For comparison, the SWV response of $3.3x10^{-4}$ M TP at bare GCE dipped in TP solution is shown (b) scan rate 255 mV s^{-1}

Fig. 4 Baseline-corrected SWV responses of dGuo and dAdo after the interaction of $3.3x10^{-4}$ M (bp) dsDNA with TP (a), $3.3x10^{-4}$ M (bp) ssDNA with TP (b), $3.5x10^{-4}$ M dAMP with TP (c) and $2.9x10^{-4}$ M dGMP with TP (d) in solution for 15 min followed by the modification of GCE surface by corresponding reaction products and SWV record in PB pH 7.4. For comparison, the SWV response of $3.3x10^{-4}$ M TP at bare GCE is shown (b, c, d) scan rate 255 mV s^{-1}

Fig. 5 UV-Vis absorption spectra of $6.1x10^{-5}$ M (bp) dsDNA in the absence of TP (red lines), in the presence of $1.1x10^{-5}$ M TP (a), $2.8x10^{-5}$ M TP (b), $5.6x10^{-5}$ M TP (c) (blue lines) and the DNA-TP mixtures (green lines); the difference spectra obtained by a software subtraction of the record for TP from the dsDNA+TP mixture records (brown lines), all in PB pH 7.4

Fig. 6 FTIR spectra of $3x10^{-3}$ M (bp) dsDNA (red line), $1x10^{-3}$ M TP (blue line) and dsDNA-TP mixture (green line), all in PB pH 7.4

Highlights:

- Bioelectrochemical approach was applied to binding interactions of nucleotides.
- Voltammetric signals indicate theophylline binding to the nucleobases.
- Theophylline at its high concentration is attached outside DNA.
- UV-Vis and FTIR spectra confirm association of theophylline with the nucleobases.
- DNA-theophylline complex structure is predicted based on hydrogen bonding.

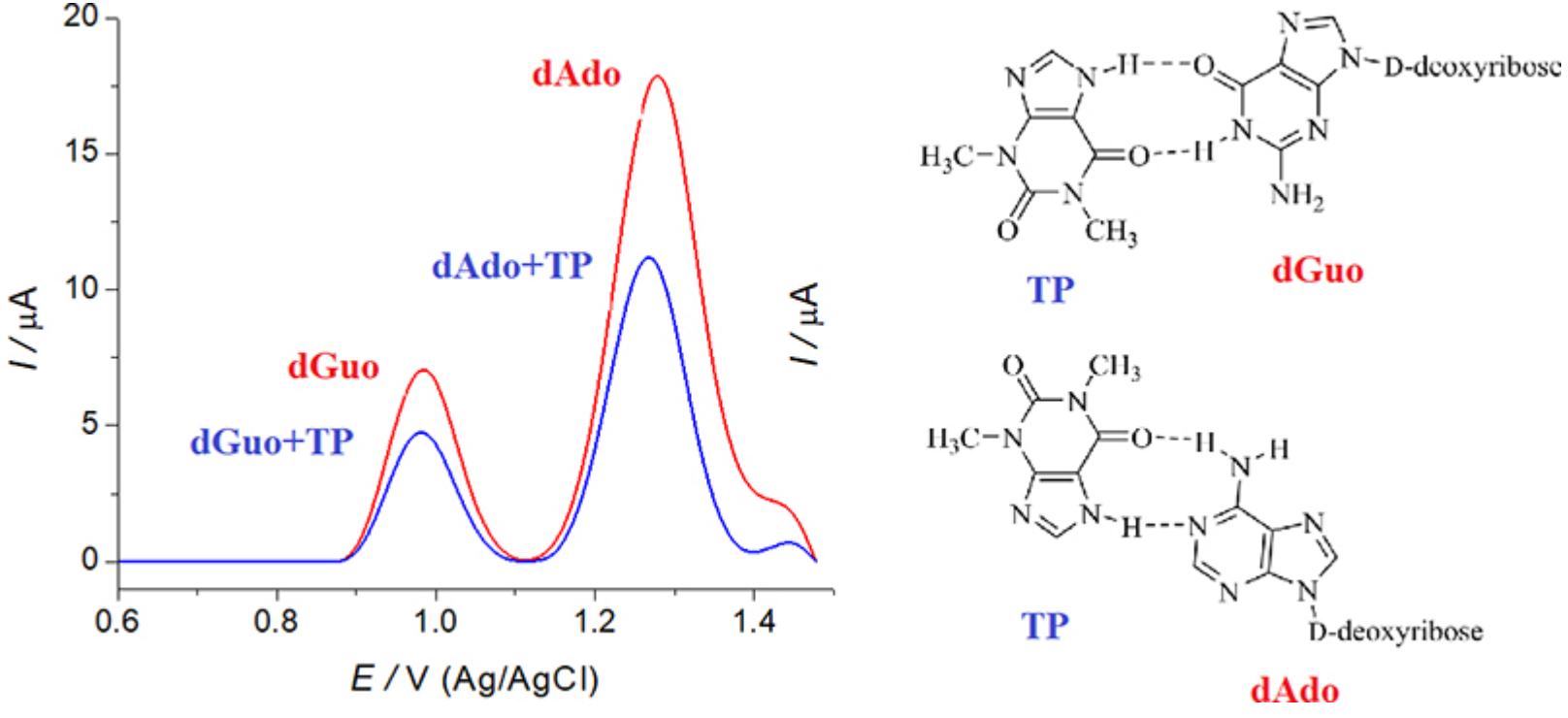

Graphics Abstract

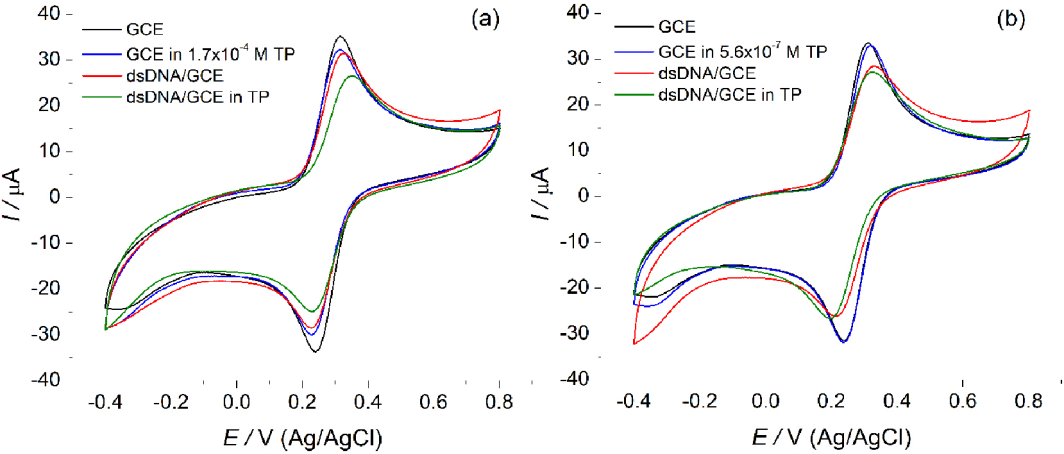
(a)
GCE
GCE in 1.7x10^{-4} M TP
dsDNA/GCE
dsDNA/GCE in TP
I / µA
E / V (Ag/AgCl)
(b)
GCE
GCE in 5.6x10^{-7} M TP
dsDNA/GCE
dsDNA/GCE in TP
I / µA
E / V (Ag/AgCl)

Figure 1

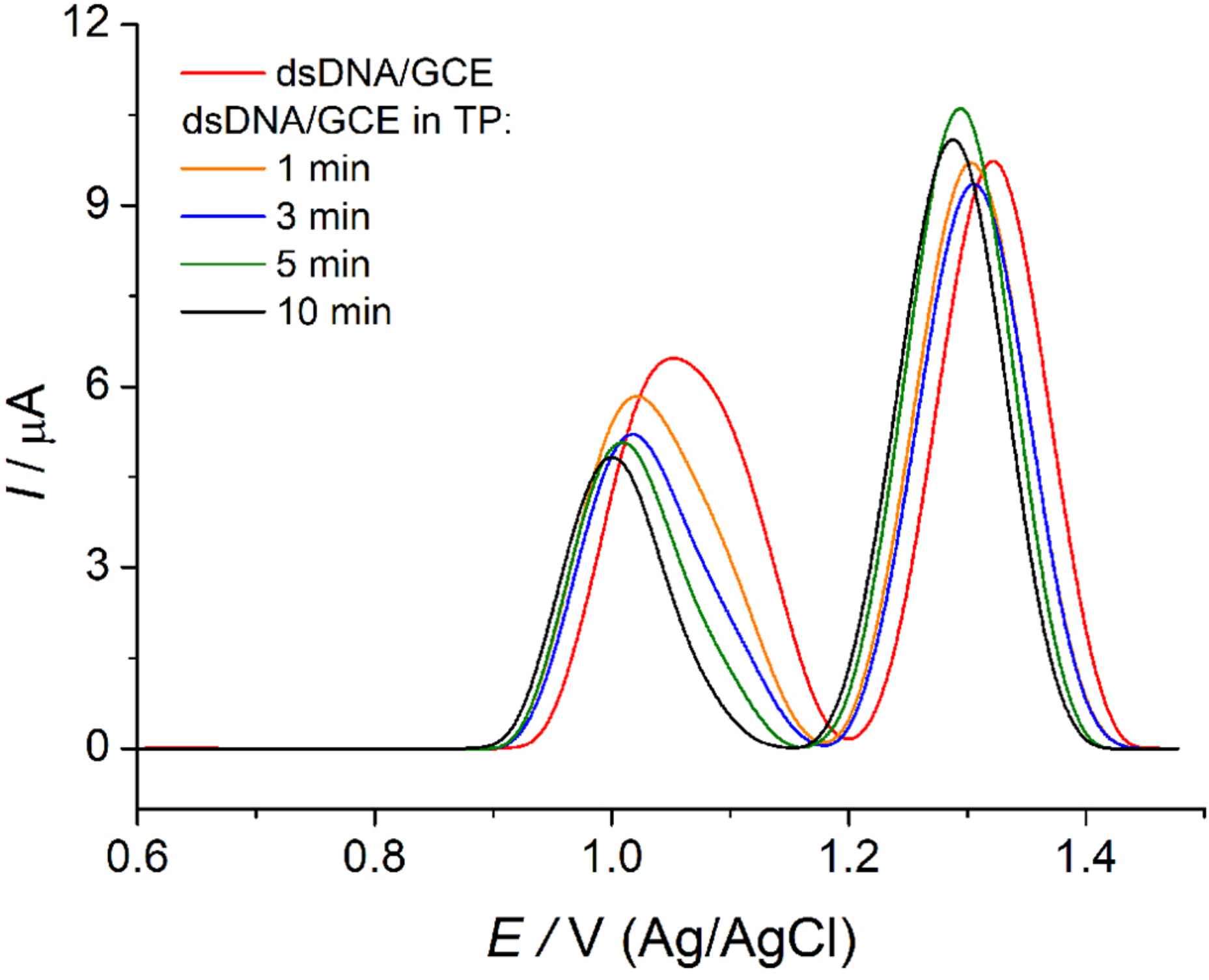
12
9
6
3
0
I / µA
dsDNA/GCE
dsDNA/GCE in TP:
1 min
3 min
5 min
10 min
0.6
0.8
1.0
1.2
1.4
E / V (Ag/AgCl)

Figure 2

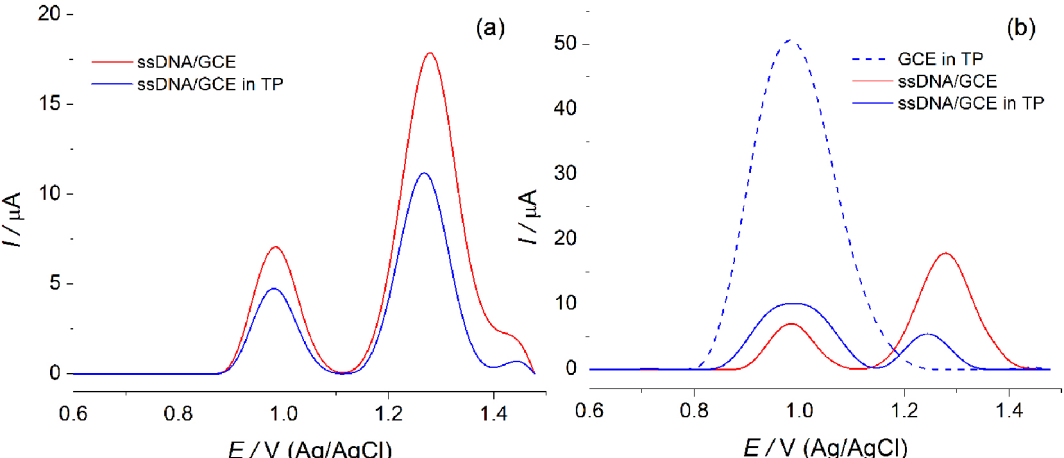
(a)
ssDNA/GCE
ssDNA/GCE in TP
I / μA
E / V (Ag/AgCl)
(b)
GCE in TP
ssDNA/GCE
ssDNA/GCE in TP
I / μA
E / V (Ag/AgCl)

Figure 3

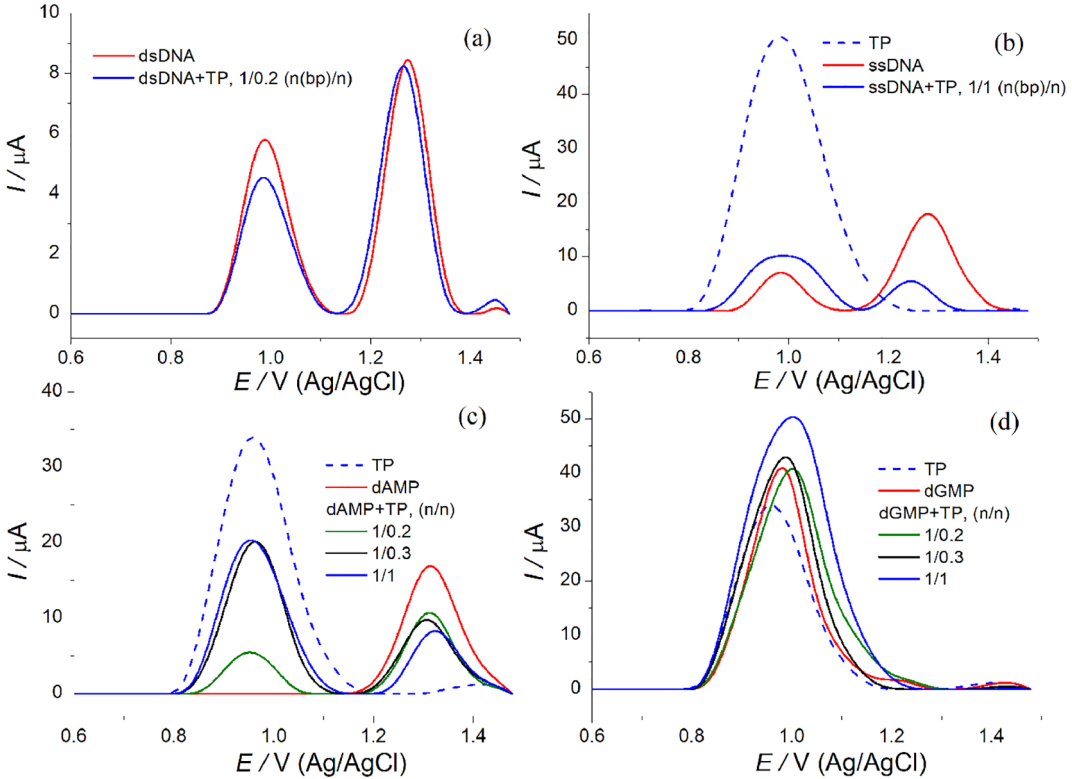
(a)
dsDNA
dsDNA+TP, 1/0.2 (n(bp)/n)
I / μA
E / V (Ag/AgCl)
(b)
TP
ssDNA
ssDNA+TP, 1/1 (n(bp)/n)
I / μA
E / V (Ag/AgCl)
(c)
TP
dAMP
dAMP+TP, (n/n)
1/0.2
1/0.3
1/1
I / μA
E / V (Ag/AgCl)
(d)
TP
dGMP
dGMP+TP, (n/n)
1/0.2
1/0.3
1/1
I / μA
E / V (Ag/AgCl)

Figure 4

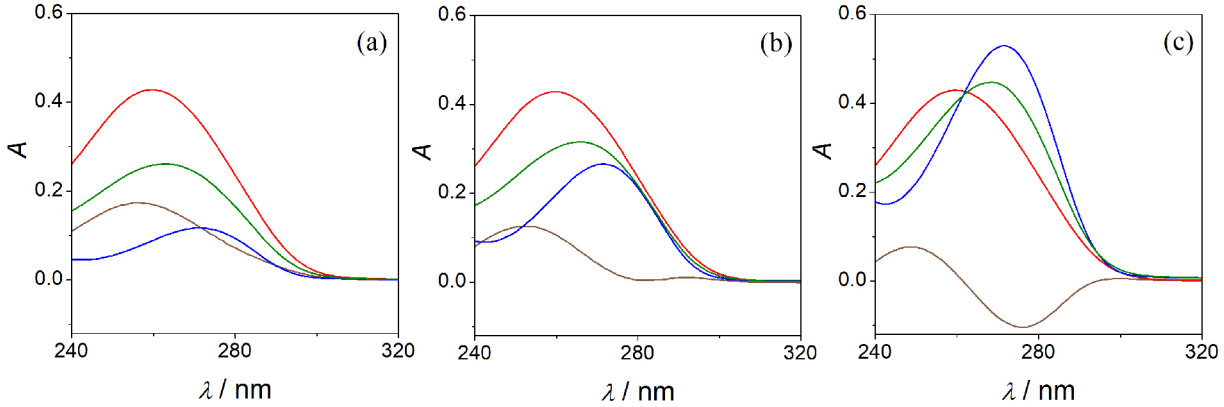

Figure 5

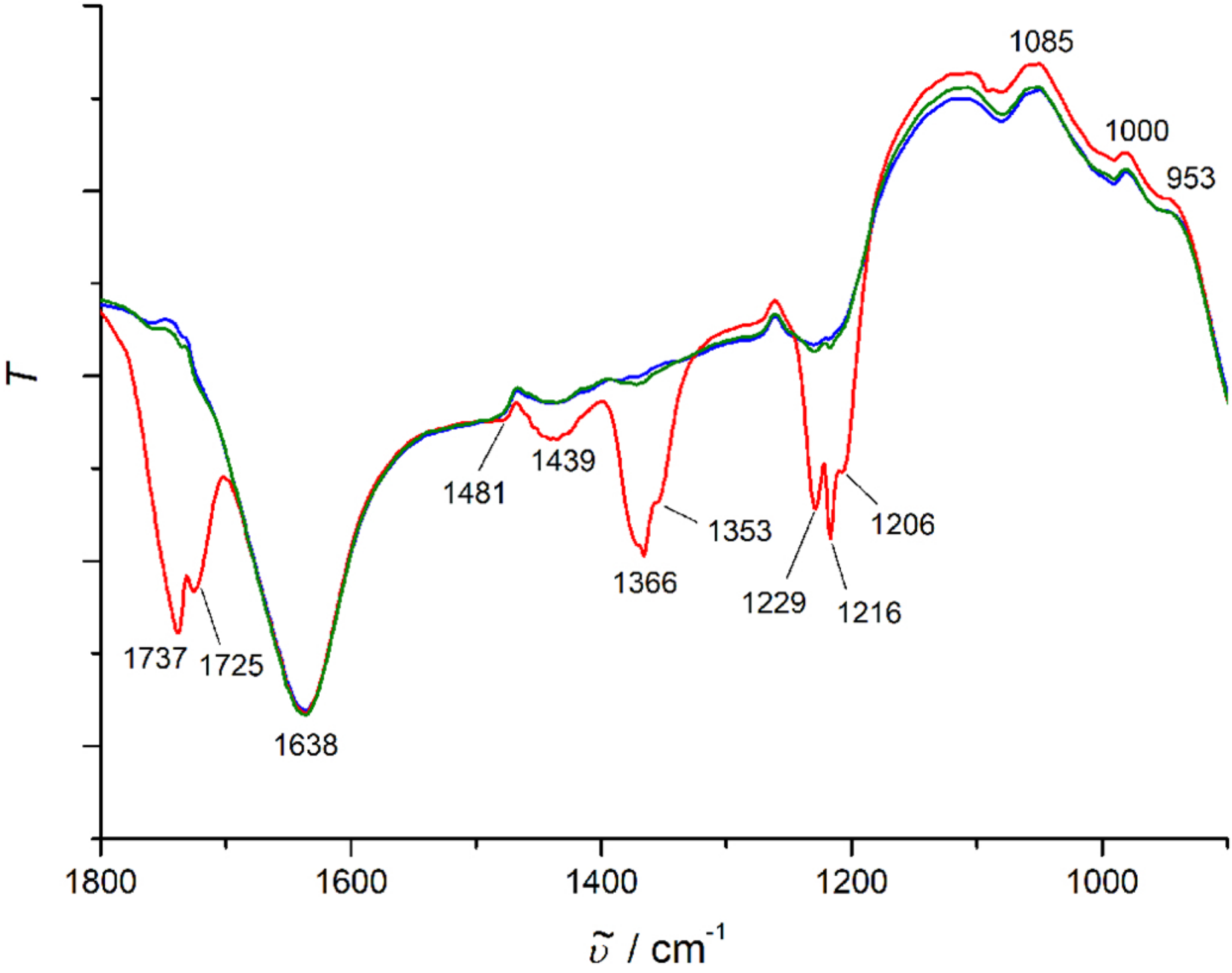
1085
1000
953
1481
1439
1353
1206
1366
1229
1216
1737
1725
1638
T
1800
1600
1400
1200
1000
$\tilde{\upsilon}$ / cm^{-1}

Figure 6